

Punching Behavior of Post-Tensioned High Strength Concrete Slabs

Mostafa S. Ragab, Kaled H. Riad and Amr H. Zaher

Department of Structural Engineering,
Faculty of Engineering, Ain Shams University, Cairo, Egypt

Abstract: The paper focuses on the strand distribution effect on punching shear strength of post-tensioned high strength concrete flat slabs supported on square columns. The punching shear behavior of 6 post tensioned slab specimens is investigated experimentally; the tested slabs had various post tensioning layouts and different concrete strength. The test results are compared to ACI, CSA, BS, CEB and ECP codes predictions. In addition, a Strut and Tie Model was applied to predict the capacity of tested post tensioned slabs. It was found that using post tensioning improved the tested slab two way shear capacity by about 17% for distributed strand layout and by about 30% for banded-distributed arrangement. Based on the comparison of codes capacity predictions with the test results, the ACI, CSA and ECP underestimate the capacity of punching shear strength. However, BS and CEB and the applied STM showed a good agreement with the test results. Further, an extensive study for more than 40 specimens from past researches was performed by applying the ACI equations to predict the punching shear strength. Modifying the critical section from $0.5d$ to $0.75d$ improved the predictions for the slab punching shear capacity of the studied specimens.

Key words: ACI • BS • CEB • Column • CSA • ECP • Flat slabs • High strength • Post-tensioned slabs • Punching shear strength • Strut-and-Tie

INTRODUCTION

High strength concrete can be obtained using ordinary cement and aggregate adding very powerful water reducing admixtures. By the new technology compressive strength of 138 MPa can be reached in cast in place buildings [1]. Flat slab systems have an advantage due to the ease of construction through the simplicity of formwork, reinforcement placement and accessibility of building utilities (Electrical ducts, Mechanical hoses and shafts, ...etc.). The time saving during construction can significantly reduce the cost of the project. In the last few decades the development of concrete production technology and practice has led to a significant change in the definition of high strength concrete, for instance in the 1950s, concrete with compressive strength (f'_c) of 35 N/mm² was considered to be high strength concrete. For present time, American Concrete Institute (ACI 318-08) ACI [2] defines the high-strength concrete as a concrete with a minimum 28-day cylinder compressive strength (f'_c) of 70 N/mm². Post-tensioning allows bigger clear spans, smaller slabs

thicknesses and fewer beams, which result a smaller amount of concrete and lower weight of the overall structure. The small slab thickness and fewer numbers of columns lead to higher column loads and bigger potential of punching failure in the slab. It is a method for acting with compression forces on concrete after casting and curing. Stages of post-tensioning procedure are; the concrete is cast around plastic, steel or aluminum curved ducts. Tendons to be set inside ducts and are tensioned by hydraulic jacks that react (push) against the concrete member itself. When tendons reach the targeted stresses, they are wedged in position and maintain tensioned after the jacks are removed, transferring pressure to the concrete [3]. The duct is then grouted to protect the tendons from corrosion. The problem of punching shear is the piercing and the main contributing factor in the design of flat slabs. The relatively abrupt nature of failure in shear, as compared to a ductile flexural failure, makes it desirable to design members so that strength in shear is relatively equal to, or greater than, strength in flexure, to ensure that a ductile flexural failure precedes shear failure.

Corresponding author: Mostafa S. Ragab, Structural Engineering Department,
Faculty of Engineering, Ain Shams University, Cairo, Egypt.

Table 1: Specimens parameters.

Slab label	Concrete grade(MPa)	Reinforcement type
SNN1	44 (Normal strength)	Normal reinforcement
SHN1	84 (High strength)	Normal reinforcement
SNP1	38 (Normal strength)	Normal reinforcement + Post tensioned steel
SHP1	82 (High strength)	Normal reinforcement + Post tensioned steel
SHP2	84 (High strength)	Normal reinforcement + Post tensioned steel
SHP3	84 (High strength)	Normal reinforcement + Post tensioned steel

Table 2: Specimens group

Group no.	Parameter	Slab Code
1	Concrete strength	SNN1,SHN1
2	Normal Concrete strength and post-tensioning	SNN1,SNP1
3	Location and distribution of cables	SHP1,SHP2,SHP3

Experimental Investigation: The experimental program of this research consisted of testing six simply-supported reinforced concrete slabs as shown in the following Table 1.

Slabs were divided into three groups according to the previous parameters taken into consideration in this investigation as shown in Table. Pre-stressing was applied by using 7 wirestraight strands with a diameter of 15.24mm (0.60"). Strands grade are 270 with ultimate strength (f_{pu}) of 1860MPa. Strands used were bonded to the surrounding concrete by grouting with cement suspension. All strands were loaded up to $(0.60f_{pu})$.

Geometry and Reinforcement of Test Slabs: The tested slabs were designed with an overall depth of 120mm and with a span of 1.3m. The bottom reinforcement of slabs was $\Phi 12$ at 100mm spacing with a percentage of normal steel of 0.57% for all specimens and with 20mm concrete cover. The concrete cover to the strand C.G. is 42mm. The top reinforcement was $\Phi 8$ at 200mm. Three different strands distributions were used. A banded-Banded distribution for SNP1 and SHP1, a distributed –distributed layout for SHP3 and a partiallybanded-distributed layout for SHP2 as shown in Fig.1.

The specimens were placed between the jack head and the steel frame and supported on four hinged line supports as shown in Fig. 2. All slabs were loaded by one concentrated load at mid span up to failure. The load was applied using a hydraulic jack and transmitted to the reinforced concrete slab on a 100mm x 100mm steel pad to provide an uniform bearing surface. Fig. 2 shows the testing setup. The load was applied gradually with constant rate of loading (20 kN load increments) during the test.

Specimens Behavior: Under loading, the cracks started with longitudinal cracks running from the mid span toward the slab edges. This was shortly followed by the formation of circumferential cracks around the load. As the load was increased, circumferential cracks occurred at a location farther away from the column stub. Inclined shear cracks appeared at approximately 50 to 65% of the ultimate punching capacity. The critical inclined shear crack developed from the top surface at an angle "0", forming the critical failure surfaces in Fig. 3 & 4.

Generally, two phases during the test were observed starting from the first shear crack up to the shear failure: the first phase was the cracking formation phase in which new diagonal shear cracks occurred and the second phase was the stabilizing cracking phase in which only the shear cracks were widening till shear failure occurred due to significant and wider shear cracks in the shear cracking zone.

Deflection Profiles: To record specimen vertical deflection, seven vertical LVDTs with 100 mm amplitude and 0.01 mm accuracy were used to measure the deflections during all stages of loading. Fig. 5 shows the load deflection curves for all specimens. The linear behavior of all specimens at all stages of loading indicates the brittle failure mode. It can be seen that high strength post tensioned slabs have higher failure loads with smaller deflection.

Effect of Strands Distribution: It is interesting to note that the first cracks in the banded specimens always started from the edges of the slab specimen where the reinforcement ratio was lower. Conversely, the first cracks in the slab specimens with the uniform distribution of reinforcement started at the column corners where the

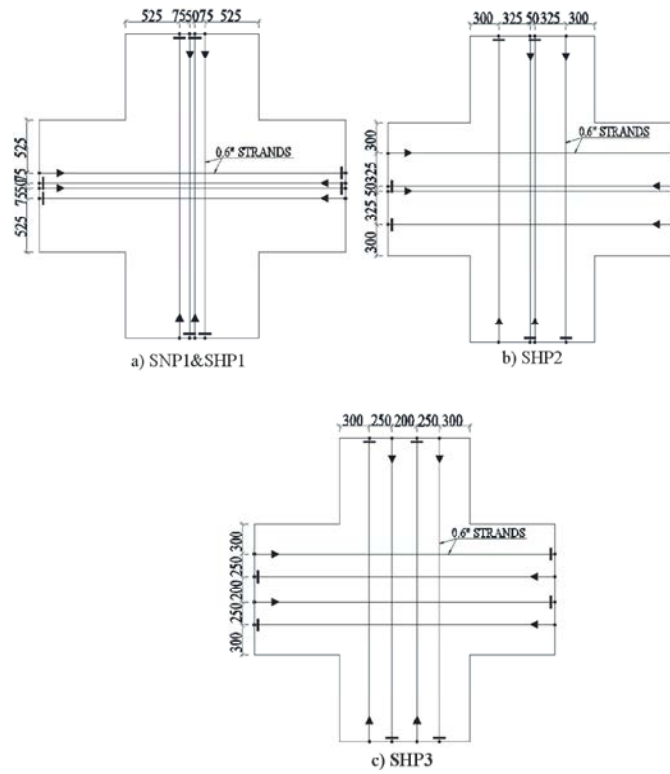


Fig. 1: Schematic arrangement of pre-stressing tendons for SNN1, SHN1, SHN2 & SHN3.

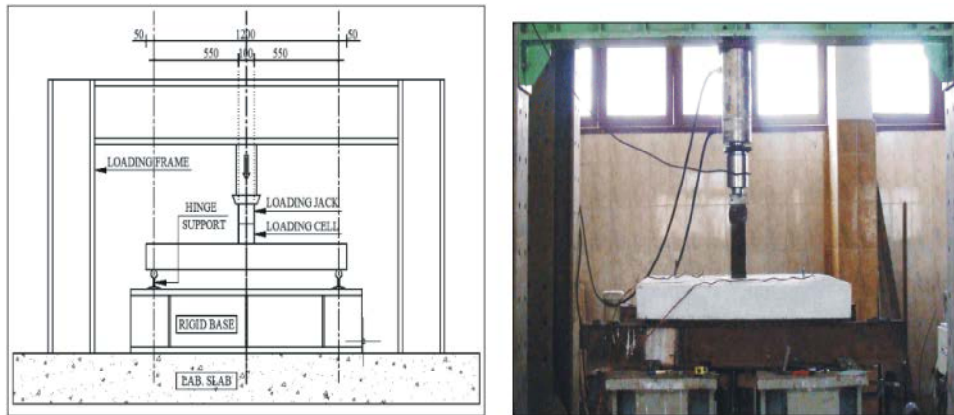


Fig. 2: Test setup

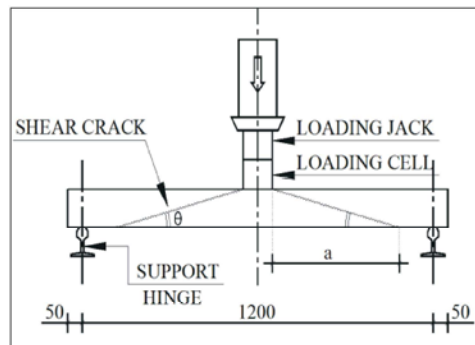


Fig. 3: Inclination angle of failure surface



Fig. 4: Crack pattern

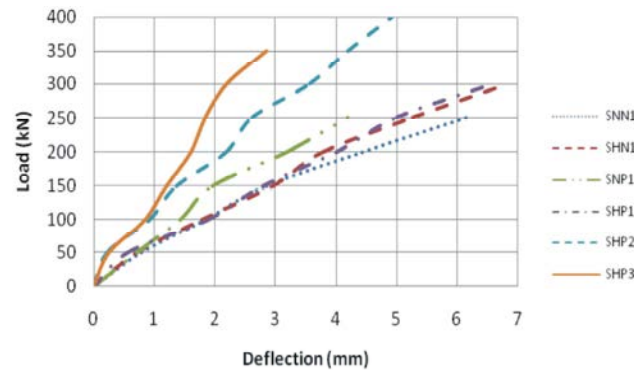


Fig. 5: Comparison between all specimens at different load stages

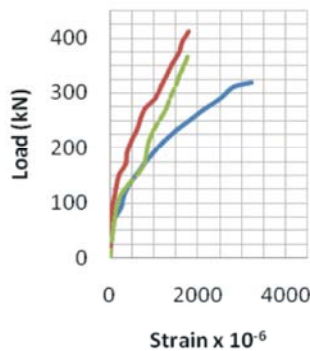


Fig. 6: Concrete strain curve for SHP1, SHP2 and SHP3

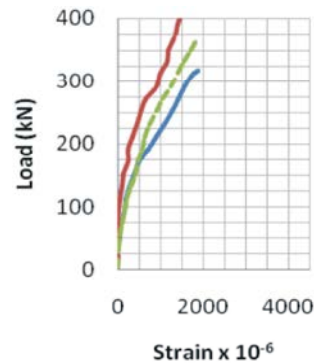


Fig. 7: Steel strain curve for SHP1, SHP2 and SHP3

stresses were the highest and then the cracks propagated towards the edges of the slab. The arrangement of strands affected the ductility of slabs. SHP2 is more ductile than SHP3, the slab sustained more load with higher deformations and deflections. Strand slippage occurred during the testing of specimen SHP1; hence its behavior was similar to the non-prestressed specimens.

The influence of the concentration of the strands in the immediate column region on the failure load and measured strains is discussed below. The failure loads for the three specimens SHP1, SHP2 and SHP3 were 337, 431 & 381 kN, respectively. Comparing the failure loads for SHP2 & SHP3, an increase in the failure load by 10% is noticed. Concrete reached strain in specimen SHP1

exceeding 0.003 but for SHP2&SHP3 the concrete did not reach that strain and reached almost the same value of strain about 0.002 Fig. 6. As mentioned before the strands slippage occurred for specimen SHP1 affected its failure load and overall behavior. Fig. 7 show steel strain curve for SHP1, SHP2 and SHP3.

Strain in Concrete and Normal Steel Reinforcement:

Before casting the specimens, electrical strain gauges with 10 mm length, 120 ohms gauge resistance and 2.07 gauge factor were provided and fixed on slab bottom reinforcement in both direction using epoxy. In addition a 100 mm strain gauge was used at the compression fibers of concrete to measure the concrete strain during the test.

Effect of Concrete Compressive Strength: From Fig. 8, it can be seen that the relation between the applied load and measured concrete strain is almost linear till failure and the maximum strain is about 0.001 for specimen SNN1. However for SHN1, the relation is linear up to strain equal to 0.0015 and the relation turn to bilinear to the failure load. From Fig. 9, the effect of post tensioning is clearly seen as the relation is turned to a bilinear one. The curve starts with a small variation of the strain with the increased loading up to 100 kN due to the pre-compression and before cracking, after cracking the strain variation increased significantly till failure. For the post-tensioned and ordinary specimens increasing the concrete strength from about 40 MPa to about 80 MPa increased the capacity by about 25%. As shown in Fig. 10, steel reached the yield strain in the normal concrete specimens SNN1 before failure which can be attributed to the dowel action behavior for this slab. The cracking loads for SNN1 and SHN1 were at 75kN & 120kN respectively. Due to the presence of the post-tensioning steel in addition to the ordinary reinforcement it can be seen in Fig. 11 that for the post-tensioned specimens the steel strains developed at all stages of loading were less than ordinary reinforcement specimens.

Punching Shear Design: The punching shear strength of a prestressed concrete slab is obtained by calculating a nominal shear stress on a critical shear perimeter at different distance away from the column. Different codes of practice recommend different equations for punching shear. That is, the treatment of prestressing effect, location of critical shear perimeter and tension reinforcement by one code can be quite different from another code. To treat prestressing effect, the ACI 318-08

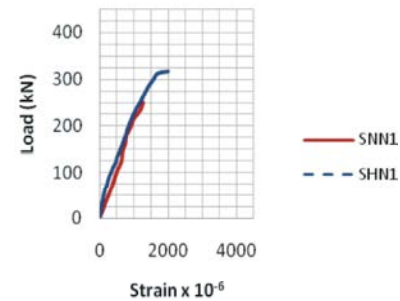


Fig. 8: Concrete strain curve for SHN1&SNN1

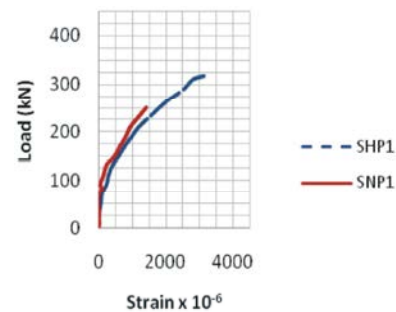


Fig. 9: Concrete strain curve for SHP1&SNP1

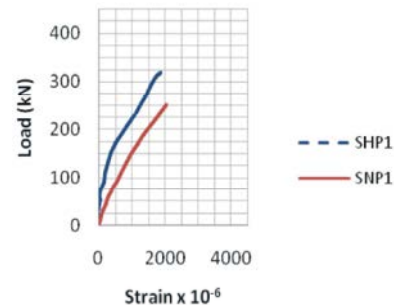


Fig. 10: Steel strain curve for SHP1&SNP1

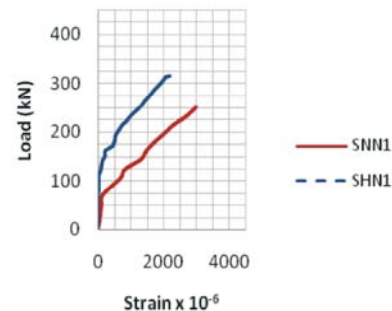


Fig. 11: Steel strain curve for SNN1&SHN1

[2], ECP-07 [4], CSA A23.3-04 [5] and EC2 [6] consider the prestressing force in term of pre-compression stress ($f_{p,c}$) in addition to the vertical component of the prestressing force (V_p). In the BS 8110-97 [7], treating the prestressing effect is completely different. The cross-sectional area of

the tendons can be replaced by an equivalent area of ordinary reinforcing steel. Then the equivalent reinforcement area is substituted into the relevant expression for the shear strength of an ordinary reinforced concrete slab. The CEB-FIP-90 [8] code defines the effect of prestress on the shear behavior of slabs as an external action-effect. The shear resistance of prestressed slabs is taken as the superposition of the load corresponding to decompression of the tension face of the slab in the vicinity of the connection and the load resisted as an ordinary reinforced concrete slab. The ACI, CSA and ECP consider the shear perimeter to be located at 0.5d away (d is the effective depth of slab) from the column face whereas BS takes it to be at 1.5d away while CEB& EC2 take it to be at 2d away from column (load) face.

ACI 318-05: The ACI code recommends that the punching shear strength around interior column in two-way prestressed slabs without shear reinforcement, to be conservatively predicted by:

$$V_c = (\beta_p \sqrt{f'_c} + 0.3 f_{p,c}) b_o d + V_p \quad (\text{SI}) \quad (1)$$

The punching shear strength of non-prestressed slabs without shear reinforcement can be determined from the lowest of the following expressions:

$$V_c = 0.33 \sqrt{f'_c} b_o d \quad (\text{SI}) \quad (2)$$

$$V_c = 0.17 \left(1 + \frac{2}{\beta} \right) \sqrt{f'_c} b_o d \quad (\text{SI}) \quad (3)$$

$$V_c = 0.083 \left(\frac{\alpha_s d}{b_o} + 2 \right) \sqrt{f'_c} b_o d \quad (\text{SI}) \quad (4)$$

where;

β_p Is the smaller of 0.29 or $0.083 \left(\frac{\alpha_s d}{b_o} + 1.5 \right)$

$f_{p,c}$ Is the average value of prestress, P/A , for the two directions. $f_{p,c}$ in each direction shall not be less than 0.86 MPa, nor be taken greater than 3.45 MPa. If $f_{p,c}$ is less than 0.86 MPa, the effect of the prestress on the nominal shear capacity of the slab is conservatively ignored and Eqs. (2) to (4) derived for ordinary reinforced concrete slabs should be applied.

f'_c Should not be taken greater than 70MPa.

V_p Is the vertical component of all effective prestress forces crossing the critical section.

β Is the ratio of the longer side to the shorter side of the concentrated load (or column)

α_s Is 40 for interior columns, 30 for edge columns and 20 for edge columns

b_o Is the length of critical shear perimeter taken at a distance of 0.5d away from the column face and has square corners for square columns and rounded corners for circular columns.

From Equations (1) to (4) above, it is clear that the ACI 318-05 method ignores the influence of flexural reinforcement and size effect on the punching shear capacity.

ECP-07: The shear resistance of a concrete flat slab in the vicinity of concentrated loads or reactions in ECP-07 is also treated in a similar procedure to the ACI code Two-way action of prestressed slabs with a critical section perpendicular to the plane of the slab and located at a distance 0.5d from the concentrated load or reaction area should be designed according to:

$$V_c = (0.27 \sqrt{f_{cu}} + 0.3 f_{p,c}) b_o d + V_p \quad (\text{SI}) \quad (5)$$

The punching shear strength of non-prestressed slabs without shear reinforcement can be determined from the lowest of the following expressions:

$$V_c = 0.316 \sqrt{f_{cu}} b_o d \quad (\text{SI}) \quad (6)$$

$$V_c = 0.316 \left(0.5 + \frac{a}{b} \right) \sqrt{f_{cu}} b_o d \quad (\text{SI}) \quad (7)$$

$$V_c = 0.8 \left(\frac{\alpha d}{b_o} + 0.2 \right) \sqrt{f_{cu}} b_o d \quad (\text{SI}) \quad (8)$$

where;

f_{cu} Is the cubic concrete strength

a Is the shorter side length of the column

b Is the longer side length of the column

α_s Is 4 for interior columns, 3 for edge columns and 2 for edge columns and the other factors are same as ACI code.

CSA-A23.3-04: The shear resistance of a concrete flat slab in the vicinity of concentrated loads or reactions in

CSA A23.3-04 is treated in a similar procedure to the ACI code Two-way action of prestressed slabs with a critical section perpendicular to the plane of the slab and located at a distance $0.5d$ from the concentrated load or reaction area should be designed according to:

$$V_c = \beta_p \lambda \sqrt{f'_c} \left(\sqrt{1 + \frac{f_{pc}}{0.33 \lambda \sqrt{f'_c}}} \right) b_o d + V_p \quad (\text{SI}) \quad (9)$$

The punching shear strength of non-prestressed slabs without shear reinforcement can be determined from the lowest of the following expressions:

$$V_c = 0.38 \sqrt{f'_c} b_o d \quad (\text{SI}) \quad (10)$$

$$V_c = 0.19 \left(1 + \frac{2}{\beta} \right) \sqrt{f'_c} b_o d \quad (\text{SI}) \quad (11)$$

$$V_c = \left(\frac{\alpha_s d}{b_o} + 0.19 \right) \sqrt{f'_c} b_o d \quad (\text{SI}) \quad (12)$$

where;

β_p Is the smaller of 0.33 or $\left(\frac{\alpha_s d}{b_o} + 0.15 \right)$

α_s Is 4 for interior columns, 3 for edge columns and 2 for edge columns and the other factors are same as ACI code.

Eurocode 2-2004: The punching shear is checked at the face of the column and at a critical section at a distance of $2d$ from the face of the support or load. The nominal design shear strength is calculated from the following equation:

$$v_{Rd,c} = \left[C_{Rd,c} K (100 \rho_l f_{ck})^{\frac{1}{3}} + k_1 \sigma_{cp} \right] \leq (v_{\min} + k_1 \sigma_{cp}) \quad (\text{SI}) \quad (13)$$

Where; $K = 1 + \sqrt{\frac{200}{d}} \leq 3$

f_{ck} Is the characteristic compressive concrete cylinder strength at 28 days, Mpa.

$k_1 = 0.15$, $C_{Rd,c} = 0.18 \gamma_c$
 $\sigma_{cp} = (\sigma_{cx} + \sigma_{cy})/2$, $\rho_l = \sqrt{\rho_{lx} \rho_{ly}} \leq 0.02$

γ_c Is a partial safety factor for concrete strength and is taken 1.50

BS 8110-97: In BS 8110-97, design concrete derived based on experimental observations, is defined as:

$$v_c = 0.79 \left(\frac{100 A_s}{b_o d} \right)^{\frac{1}{3}} \left(\frac{400}{d} \right)^{\frac{1}{4}} \left(\frac{f_{cu}}{25} \right)^{\frac{1}{3}} \quad (\text{SI}) \quad (14)$$

where;

$\frac{A_s}{b_o d}$ Is the flexural reinforcement plus the tendons equivalent reinforcement ratio

$\frac{400}{d}$ Is the size effect factor which should not be taken less than 1.0

f_{cu} Should not be taken greater than 40 MPa.

The ultimate punching shear load V_u can then be obtained from

$$V_u = v_c b_o d \quad (\text{SI}) \quad (15)$$

where V_u is the ultimate design shear force, b_o is the effective shear perimeter. BS 8110 uses a shear perimeter at $1.5d$ away from the column face and has square corners regardless of the shape of the column. BS 8110 also recommends an upper limit for the shear resistance expressed in terms of the shear stress at the periphery of the loaded area. The shear stress v at the periphery of the loaded area has to be less than the smaller of $0.8 \sqrt{f_{cu}}$ or 5 N/mm^2 .

CEB-FIP-90: The shear resistance of prestressed slabs taken at a control perimeter of a distance $2d$ from the periphery of a column or concentrated load is recommended by CEB-FIP-90 code in a form of:

$$v_c = 0.12 \xi (100 \rho f_{ck})^{1/3} \quad (\text{SI}) \quad (16)$$

where;

$$\xi = 1 + \sqrt{\frac{200}{d}} \quad (17)$$

The ultimate punching shear load V_u can then be obtained from

$$V_u = v_c b_o d \quad (18)$$

The reinforcement ratio may be calculated as the average for two orthogonal directions. In each direction

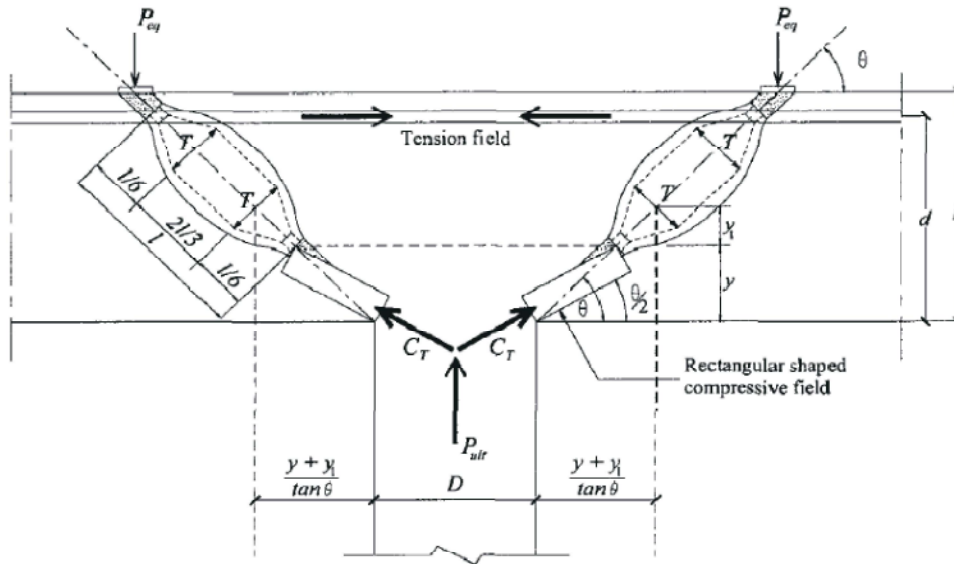


Fig. 12: Refined strut and tie model for symmetric punching of concrete slab

the effective width in the calculation of ρ is equal to the side dimension of the column plus $3d$ to the either side of it. Bonded prestressing tendons can be included in the calculation of ρ but un-bonded tendons should be excluded. The effective depth of the slab is assumed constant and may normally be taken as that to the mean plane of an orthogonal arrangement of tension reinforcement, but f_{ck} should be limited to less than 50 Mpa.

Strut and Tie Model for Symmetric Punching of Concrete Flat Slabs: Punching of slabs generates when failure in the ultimate zone occurs by high concrete compression stress. For normal strength concrete, the angle of inclination θ has been experimentally determined to be between 26 and 30 degrees, whereas for high strength concrete the angle varies between 32 and 38 degrees as determined through experimental testing by Marzouk and Hussein [9]. As shown in Fig. 12, these previous ranges were already observed in this research and all inclination angles for all specimens are shown in Table 3. The following equation is proposed by Risk [10] to determine the punching shear capacity of normal reinforced concrete slabs.

$$P_{ult} = \left[\pi \left(D + \frac{2y}{\tan \theta} \right) (I_{ch}/h)^{0.33} \frac{y \sin \theta / 2}{\sin \theta} \right] f_{c2, \max} \sin \theta / 2 \quad \text{N (SI)} \quad (19)$$

where;

$$f_{c2, \max} = \frac{\lambda \phi_c f_c}{0.8 + 170 \epsilon_1} \leq \phi_c f_c \quad \text{MPa (SI)} \quad (20)$$

D Is the diameter of column, a square column can be replaced in the equation by an equivalent circular column with the same perimeter $D=4C/\pi$

I_{ch} Is the characteristic length, h is the section height.

$$y = \frac{A_s f_y}{0.85 f_c b} = \frac{\rho d f_y}{0.85 f_c} \quad \text{For non prestressed concrete}$$

$$y = \frac{A_{ps} f_{ps} + A_s f_y}{0.85 f_c b} \quad \text{For prestressed concrete}$$

Table 4 summarizes the shear capacity predictions for all tested slabs using the above mentioned international codes and STM. Moreover, the shear capacities obtained from this experimental investigation are shown in Table 4.

Table 5 summarizes the comparison between the experimental punching shear capacity and predictions using the current international codes " $V_{test}/V_{predicted}$ ". For group 1, applying BS8110 equations gives a good estimation for the failure punching loads. It is obvious that all other codes are conservative and underestimating the shear strength. In addition, it is clear that results obtained from CEB and EC are similar. For group 2, the gap between actual to predicted shear strength increased using ACI318 and ECP-2007. However, for the CEB predicted failure loads are more accurate. EC2 is overestimating the punching shear load. ACI, ECP and CSA are more consistent in the variation of results. For group 3, the effect of prestressing steel passing through the critical perimeter is well considered in CEB

Table 3: Failure load and shear crack inclination angle

Slab label	f_{cu} (MPa)	A (mm)	θ (deg.)	Failure Load (kN)
SNN1	44.30	230	28	250.10
SHN1	83.70	200	31	325.90
SNP1	37.60	210	30	271.00
SHP1	81.90	180	34	337.00
SHP2	83.70	160	37	431.00
SHP3	83.70	150	39	381.00

Table 4: Values of test and predicted failure loads for test results, code results & STM.

Slab label	f_c Mpa	f_{pc} MPa	Test result (kN)	ACI318-2008 (kN)	BS8110-1 (kN)	CSA A23.3-04 (kN)	ECP-2007 (kN)	CEB-FIP (kN)	EC2- 2004 (kN)	STM (kN)
SNN1	35.44	0.00	250.10	143.30	226.59	165.01	153.42	204.04	204.04	230.09
SHN1	66.96	0.00	325.90	196.98	280.12	226.82	210.88	252.25	252.25	345.85
SNP1	30.08	2.03	271.00	127.62	201.79	176.61	131.40	272.41	313.75	222.37
SHP1	65.52	2.48	337.00	179.32	249.54	249.58	184.90	353.12	403.58	367.38
SHP2	66.96	2.39	431.00	179.25	252.16	249.75	184.88	300.87	349.50	375.46
SHP3	66.96	2.39	381.00	179.25	252.16	249.75	184.88	300.87	349.50	375.46

Table 5: Ratio between test results, code results & STM.

Slab label	$V_{test}/V_{predicted}$						
	ACI318-2008	BS8110-1	CSA-A23.3-04	ECP-2007	CEB-FIP	EC2- 2004	STM
SNN1	1.75	1.10	1.52	1.63	1.23	1.23	1.09
SHN1	1.65	1.16	1.44	1.55	1.29	1.29	0.94
SNP1	2.12	1.34	1.53	2.06	0.99	0.86	1.22
SHP1	1.88	1.35	1.35	1.82	0.95	0.84	0.92
SHP2	2.40	1.71	1.73	2.33	1.43	1.23	1.15
SHP3	2.13	1.51	1.53	2.06	1.27	1.09	1.01
Average	1.99	1.36	1.51	1.91	1.19	1.09	1.05
Standard deviation	0.28	0.22	0.13	0.30	0.18	0.20	0.12
C.O.V.	14.09%	16.38%	8.25%	15.58%	15.43%	18.16%	11.20%

Table 6: Test data used for the analytical study

Slab	Support size mm	f_c MPa	f_{pc} MPa	V_p kN	h mm	d mm	P %	V_u kN
Experimental								
SNP1	100 square	30.1	2.03	0	120	80	1.4	271
SHP1	100 square	65.5	2.48	0	120	80	1.4	337
SHP2	100 square	67	2.39	0	120	80	1.4	431
SHP3	100 square	67	2.39	0	120	80	1.4	381
Eid[11]								
S1	100 square	30.1	2.03	0	120	80	1.4	260
S2	100 square	29.6	2.01	0	120	80	1.4	220
S3	100 square	29.6	1.65	0	120	80	1.4	170
Slab	Support size mm	f_c MPa	f_{pc} MPa	V_p kN	h mm	d mm	P %	V_u kN
Silva [12]								
A1	100 square	37.8	3.31	9	125	102	0.62	380
A2	100 square	37.8	2.14	10	125	108	0.47	315
A3	100 square	37.8	3.16	0	125	102	0.62	352.7
A4	100 square	37.8	1.98	0	125	103	0.51	321
B1	200 square	40.1	3.39	32.4	125	108	0.6	582.5
B2	200 square	40.1	2.23	29.9	125	105	0.48	488
B3	200 square	40.1	3.12	12.6	125	102	0.63	519.8
B4	200 square	40.1	2.16	12.5	125	100	0.5	458.8
C1	300 square	41.6	3.33	40.5	125	105	0.61	720

Table 6: Continued

C2	300 square	41.6	2.26	35.4	125	100	0.5	556.7
C3	300 square	41.6	3.48	17.7	125	100	0.64	636.6
C4	300 square	41.6	2.31	15.4	125	98	0.52	497.1
D1	200 square	44.1	3.34	10	125	99	0.68	497.1
D2	200 square	44.1	2.23	12.1	125	101	0.5	385.2
D3	200 square	44.1	2.27	0	125	100	0.51	395.2
D4	300 square	44.1	2.22	39.9	125	106	0.48	531.5
Correa [13]								
LP2	150 square	52.4	2.19	0	130	104	1.17	355
LP3	150 square	52.4	4.28	0	130	104	1.17	415
LP4	150 square	50.7	0.8	7.6	130	104	1.17	390
LP5	150 square	50.7	1.33	13	130	104	1.17	475
LP6	150 square	52.4	1.76	11	130	104	1.17	437
Kordino and Nolting [14]								
V1	φ200	33.6	1.7	65.7	150	124	0.62	450
V2	φ200	36	1.66	60.6	150	123	0.9	525
V3	φ200	36	3.09	115.6	150	122	0.62	570
V6	φ200	30.4	1.77	0	150	120	0.62	375
V7	φ200	31.2	1.77	67.5	150	124	0.62	475
V8	φ200	35.2	1.77	70.3	150	124	0.62	518
Hassanzadeh [15]								
A1	φ250	31	2.79	41.6	220	150	0.18	668
A2	φ250	28.7	2.74	0	220	146	0.18	564
B2	φ250	43.8	2.12	0	220	176	0.29	827
B3	φ250	41.1	2.21	53.5	220	190	0.29	1113
B4	φ250	43.2	1.99	0	220	190	0.29	952
Shehata [16]								
SP1	150 square	36.5	3.94	18.5	175	140	0.27	988
SP2	150 square	41.7	4.81	21	175	140	0.27	884
SP3	150 square	40.9	3.28	0	175	140	0.27	780
SP4	150 square	42.5	3.5	0	175	140	0.27	728
Melges[17]								
M4	180 square	51.9	1.95	0	160	128	0.92	773

Table 7: Results for the study using ECP-2007 equations

Slab	ACI (0.5d)		Proposed (0.75d)		Proposed (0.8d)		Proposed (0.9d)		Proposed (d)	
	V _c kN	V _w /V _c	V _c kN	V _w /V _c	V _c kN	V _w /V _c	V _c kN	V _w /V _c	V _c kN	V _w /V _c
Experimental										
SNP1	128	1.95	156	1.60	162	1.54	173	1.45	185	1.35
SHP1	179	1.88	219	1.54	227	1.48	243	1.39	259	1.30
SHP2	179	2.40	219	1.97	227	1.90	243	1.77	259	1.66
SHP3	179	2.13	219	1.74	227	1.68	243	1.57	259	1.47
Eid [11]										
S1	128	2.04	185	1.41	173	1.50	162	1.61	156	1.67
S2	98	2.24	149	1.48	139	1.58	130	1.69	126	1.75
S3	77	2.21	109	1.56	102	1.67	95	1.78	92	1.85
Silva [12]										
A1	238	1.60	296	1.29	307	1.24	330	1.15	353	1.08
A2	228	1.38	284	1.11	296	1.06	318	0.99	341	0.92
A3	225	1.57	282	1.25	293	1.20	316	1.12	339	1.04
A4	199	1.61	249	1.29	259	1.24	279	1.15	300	1.07
B1	412	1.41	479	1.22	492	1.18	519	1.12	545	1.07
B2	351	1.39	406	1.20	417	1.17	439	1.11	461	1.06
B3	354	1.47	412	1.26	423	1.23	447	1.16	470	1.11
B4	311	1.48	360	1.27	370	1.24	390	1.18	410	1.12

Table 7: Continued

C1	529	1.36	592	1.22	605	1.19	630	1.14	655	1.10
C2	443	1.26	494	1.13	504	1.10	525	1.06	545	1.02
C3	484	1.32	542	1.17	554	1.15	577	1.10	601	1.06
C4	415	1.20	465	1.07	474	1.05	494	1.01	514	0.97
D1	357	1.39	414	1.20	426	1.17	448	1.11	471	1.05
D2	328	1.18	381	1.01	391	0.98	412	0.93	434	0.89
D3	313	1.26	365	1.08	375	1.05	396	1.00	417	0.95
D4	486	1.09	544	0.98	556	0.96	579	0.92	603	0.88
Correa [13]										
LP2	291	1.22	351	1.01	363	0.98	387	0.92	410	0.86
LP3	357	1.16	431	0.96	445	0.93	475	0.87	504	0.82
LP4	251	1.55	301	1.30	311	1.25	331	1.18	351	1.11
LP5	273	1.74	327	1.45	337	1.41	359	1.32	380	1.25
LP6	289	1.51	345	1.27	357	1.22	380	1.15	402	1.09
Kordino and Nolting [14]										
V1	342	1.32	395	1.14	406	1.11	427	1.05	448	1.00
V2	340	1.55	393	1.34	404	1.30	425	1.24	446	1.18
V3	445	1.28	507	1.12	519	1.10	544	1.05	569	1.00
V6	257	1.46	305	1.23	315	1.19	334	1.12	353	1.06
V7	339	1.40	391	1.22	401	1.18	422	1.13	443	1.07
Hassanzadeh [15]										
A1	503	1.33	590	1.13	607	1.10	642	1.04	677	0.99
A2	431	1.31	511	1.10	527	1.07	558	1.01	590	0.96
B2	602	1.37	726	1.14	751	1.10	800	1.03	850	0.97
B3	716	1.56	859	1.30	887	1.25	944	1.18	1001	1.11
B4	657	1.45	799	1.19	827	1.15	884	1.08	941	1.01
Shehata [16]										
SP1	495	2.00	610	1.62	633	1.56	679	1.46	725	1.36
SP2	559	1.58	689	1.28	715	1.24	767	1.15	819	1.08
SP3	461	1.69	572	1.36	595	1.31	639	1.22	684	1.14
SP4	478	1.52	593	1.23	616	1.18	662	1.10	708	1.03
Melges [17]										
M4	422	1.83	509	1.52	527	1.47	562	1.38	597	1.29
Average	--	1.55	--	1.28	--	1.25	--	1.19	--	1.14
St. of dev.	--	0.31	--	0.21	--	0.21	--	0.22	--	0.23
C.O.V.	--	20%	--	16%	--	17%	--	19%	--	21%
Over-estimated%	--	0%	--	4.5%	--	9.0%	--	11.4%	--	22.7%

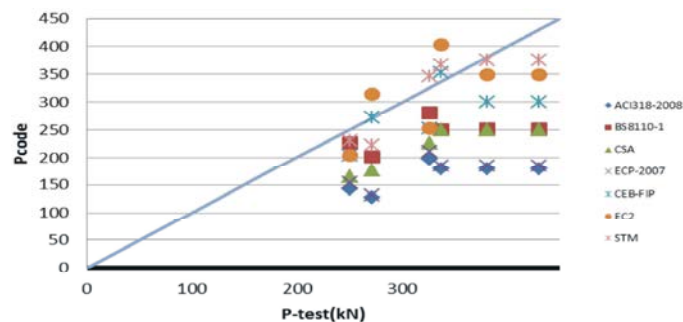


Fig. 13: Compilation of results

code, while EC is overestimating it. However BS takes the effect of prestressing steel into consideration but still underestimates its effect.

Based on all previous results a comparison between the ratio of test results with codes results and Strut and

Tie results is shown in Fig. 13 by using the STM described before, the model for estimating the punching shear strength agreed very well with the experimental results. Capacities obtained from STM have an average value of 1.05 which is very close to the actual loads.

Comprehensive Study for ACI318-08: To provide an adequate basis for comparing test data with the predictions of ACI equations, the results of the present experimental work, which was described previously, have been combined with test data available past researches. All of the results considered are for punching failures of post-tensioned slabs with bonded or unbounded tendons and bonded deformed reinforcing bars with $f_y \leq 600$ MPa. The bars were uniformly spaced across the full widths of the test slabs. The present and recent researches data are shown in Table 5. Based on ACI equations, the punching shear capacity for all specimens was generally underestimated. However, changing the position of the critical section to be at 0.75d instead of 0.5d to predict the shear failure load introduces better predictions.

CONCLUSIONS

The present study showed that post-tensioning can be successful for increasing the ultimate carrying capacity, strength, ductility and stiffness of high strength slab-column connections. The conclusions derived from the current research are as follow:

- The first cracks in the banded specimens always started from the edges of the slab specimen where the reinforcement ratio was lower. Conversely, the first cracks in the slab specimens with the uniform distribution of reinforcement started at the column corners where the stresses were the highest and then the cracks propagated towards the edges of the slab.
- Increasing slab concrete strength with 100% improved the punching shear capacity by 30.30% for normal reinforced concrete slab-column connection and 24.35% for post-tensioned slab.
- Test specimens were loaded up to failure and the critical sections were located between 1.5d to 2.3d, with critical shear inclinations angle of 31° for PNSC and 34° for PHSC specimens. These inclination angles are matching with Hegger *et al.* [18, 17] results and conclusions.
- The results obtained from ACI, CSA, ECP, EC2, BS and CEB confirmed that the conclusions of Yang *et al.* [19], that ACI, CSA and ECP generally underestimate the punching shear capacities, while applying EC2, BS and CEB gives better predictions as noticed from self-performed and test data available in the literature.

- EC2 gives the best predicted capacities for normal strength concrete specimens and agrees with the observations of Heinzmann [20] and Guandalini [21], but it overestimated the shear capacity for high strength concrete specimens.
- Despite of long equations and complexity, the applied Strut and Tie model was very close for the prediction of punching shear capacity of tested flat slabs specimens.
- According to the analysis made for more than 40 specimens, it was found that by assuming the critical perimeter at a distance 0.75d instead of 0.5d, ACI318-08 predictions are closer to the experimentally obtained capacities.

REFERENCES

1. Tom Bagsarian, 2009. High-Strength Concrete, A Historical background. A Practical Guide, First Published 2009 In the USA and Canada.
2. ACI Committee 318, 2008. Building Code Requirements for Structural Concrete (ACI 318-08) and Commentary (ACI 318M-08). American Concrete Institute, Farmington Hills, Michigan, 2008.EN 1992-1-1: 2004.
3. Amlan K. Sengupta and Devdas Menon, 2012. Prestressed Concrete Structures. Indian Institute of Technology Madras, India.
4. Egyptian Code of Practice, 2007. Egyptian Code for Designing and Construction Reinforced Concrete Structure. Ministry of Housing and Infrastructures, Cairo, Egypt.
5. The Canadian Code CSA A23.3-04, 2004. Design of Concrete Structures. Canadian Standards Association, Rexdale, Ontario, Canada.
6. CEB-FIP MC90 Model Code, 1990. Model Code For Concrete Structures. Comintary International du Beton et Federation International de la Precontrainte, Lausanne, Switzerland, pp: 437.
7. Eurocode 2, 2004. Design of Concrete Structures. Part 1-1: General Rules and Rules for Buildings, European Committee for Standardization, Brussels, Belgium.
8. British Standard BS-8110, 1997. Structural Use of Concrete. British Standard Institution, London.
9. Marzouk, H. and A. Hussein, 1991. Experimental investigation on the behavior of high strength concrete slabs. ACI Structural Journal, 88(6): 701-713.

10. Rizk, E.R.M., 2010. Structural behavior of thick concrete plates. Ph.D Dissertation, Faculty of Engineering and Applied Science Memorial University of New Foundland, Canada.
11. Eid, H., 2013. Effect of near column opening on punching behavior of post tensioned slabs. A Thesis Submitted in partial fulfillment for the requirements of the Degree of Master of Science in civil engineering (Structural), Faculty of Engineering, Ain Shams University, Cairo.
12. Ricardo, J.C. Silva, Paul E. Regan and Guilherme S.S.A. Melo, 2007. Punching of post-tensioned slabs-tests and codes. *ACI Structural Journal*, 104(2): 123-132.
13. Corrêa, G. S. 2001. Puncionamentoemlajescogumeloprotenhidas com cabos não aderentes. MSc dissertation, Department of Civil and Environmental Engineering, University of Brasília, Brazil, pp: 153.
14. Kordina, K. and D. Nölting, 1986. Tragfähigkeit durchstanzgefährdeter stahlbetonplatten. Deutscher Ausschuss für Stahlbeton, Berlin, Germany, pp: 60.
15. Hassanzadeh, G., 1998. Betongplattor på pelare, dimensionerings metoder för plattor med icke vidhäftande spännarmering. TRITA-BKN Bulletin 43, Institutionen För Byggnadskonstruktion, Kungl-Tekniska Högskolan, Stockholm, Sweden, pp: 110-130.
16. Shehata, I.A., 1982. Punching of prestressed and non-prestressed reinforced concrete flat slabs. MPhil Thesis, Polytechnic of Central London, London, pp: 336.
17. Melges, J.L.P., 2000. Análise experimental da punção em lajes de concreto armado e protendido. PhD Eng Thesis, Escola de Engenharia de São Carlos, Universidade de São Paulo, São Carlos, Brasil, pp: 350.
18. Hegger, J., M. Ricker and A.G. Sherif, 2009. Punching strength of reinforced concrete footings. *ACI Structural Journal*, 106(5): 706-716.
19. Yang, J., Y. Yoon, W. Cook and D. Mitchell, 2010. Punching shear behavior of two-way slabs reinforced with high-strength steel. *ACI Structural Journal*, 107(4): 468-475.
20. Heinzmann, D., S. Etter, S. Villiger and T. Jaeger, 2012. Punching tests on reinforced concrete slabs with and without shear reinforcement. *ACI Structural Journal*, 109(6): 787-794.
21. Guandalini, S., O.L. Burdet and A. Muttoni, 2009. "Punching tests of slabs with low reinforcement ratios. *ACI Structural Journal*, 106(1): 87-95.